Fungal Genetics and Biology 47 (2010) 855–868

Contents lists available at ScienceDirect

Fungal Genetics and Biology

journal homepage: www.elsevier.com/locate/yfgbi

Genes encoding a striatin-like protein (*ham-3*) and a forkhead associated protein (*ham-4*) are required for hyphal fusion in *Neurospora crassa*

Anna R. Simonin [1], Carolyn G. Rasmussen [1,2], Mabel Yang, N. Louise Glass *

Department of Plant and Microbial Biology, 111 Koshland Hall, University of California, Berkeley, CA 94720-3102, United States

ARTICLE INFO

Article history:
Received 31 March 2010
Accepted 16 June 2010
Available online 1 July 2010

Keywords:
Cell fusion
Neurospora
Striatin
Far complex
Forkhead associated (FHA) protein
STRIPAK

ABSTRACT

Cell–cell fusion during fertilization and between somatic cells is an integral process in eukaryotic development. In *Neurospora crassa*, the hyphal anastomosis mutant, *ham-2*, fails to undergo somatic fusion. In both humans and *Saccharomyces cerevisiae*, homologs of *ham-2* are found in protein complexes that include homologs to a striatin-like protein and a forkhead-associated (FHA) protein. We identified a striatin (*ham-3*) gene and a FHA domain (*ham-4*) gene in *N. crassa*; strains containing mutations in *ham-3* and *ham-4* show severe somatic fusion defects. However, *ham-3* and *ham-4* mutants undergo mating-cell fusion, indicating functional differences in somatic versus sexual fusion events. The *ham-2* and *ham-3* mutants are female sterile, while *ham-4* mutants are fertile. Homozygous crosses of *ham-2*, *ham-3 and ham-4* mutants show aberrant meiosis and abnormally shaped ascospores. These data indicate that, similar to humans, the HAM proteins may form different signaling complexes that are important during both vegetative and sexual development in *N. crassa.*

1. Introduction

Cell signaling resulting in cell–cell fusion is integral to a multitude of eukaryotic processes. Examples include fertilization of an egg by sperm and osteoclast development in mammals (Primakoff and Myles, 2007; Vignery, 2008; Zeng and Chen, 2009), pollen tube and ovary fusion in plants (Higashiyama et al., 2003), and the development of filamentous colonies of fungi (Buller, 1933; Fleissner et al., 2008; Read et al., 2010). Unlike unicellular yeasts, such as *Saccharomyces cerevisiae* or *Schizosaccharomyces pombe*, where cell fusion is only associated with mating, in filamentous fungi, cell fusion also occurs between vegetative cells. Somatic cell fusion is important in colony establishment and development of the interconnected hyphal network characteristic of these organisms. Connectivity in fungal networks is presumed to be necessary for maintaining proper intercolony communication, resource exploitation, virulence in pathogens, and maintaining homeostasis (Reviewed in Read et al. (2010), Fleissner et al. (2008), Glass et al. (2004), Rayner (1991) and Rayner (1996)).

A number of mutants deficient in hyphal fusion and/or signaling have been characterized in the filamentous ascomycete fungus, *Neurospora crassa* (Read et al., 2010). Many of these mutants have a decreased growth rate and are female sterile. One gene required for vegetative and germling fusion in *N. crassa* is *ham-2*, which encodes a protein with multiple transmembrane domains and a C-terminal domain of unknown function that is conserved in fungi and animals, but not in plants (Xiang et al., 2002). The *ham-2* mutant does not form conidial anastomosis tubes (CATs) and neither attracts nor responds to the presence of a wild-type germling (Roca et al., 2005).

Homologs of *ham-2* have been identified in protein complexes in both yeast and humans. Far11, a protein encoded by the *S. cerevisiae* homolog of *ham-2*, was shown to be part of a complex composed of Far3, Far7, Far8, Far9 and Far10 (Kemp and Sprague, 2003; Uetz et al., 2000). Far proteins are required for maintenance of G1 cell cycle arrest after pheromone stimulation (Kemp and Sprague, 2003). In humans, homologs of *ham-2* have been identified in a complex that acts as a regulatory subunit to protein phosphatase 2A (PP2A), and which also includes a protein similar to Far8 (striatin), and a protein similar to Far9/10 (similar to sarcolemmal membrane-associated protein, SLMAP) which contains a forkhead-associated domain (Goudreault et al., 2008). In addition, this complex contains a MOB3 homolog. Intriguingly, *mob-3* mutants were shown to be hyphal fusion mutants in *N. crassa* (Maerz et al., 2009).

In addition to *ham-2*, a genome wide search revealed that only two additional homologs to the *S. cerevisiae FAR* genes were present in the *N. crassa* genome (Glass et al., 2004), a homolog of *FAR8* (similar to striatin) and a homolog of *FAR9/10* (SLMAP). No homologs of *FAR3* or *FAR7* were identified. In this study, we

* Corresponding author. Fax: +1 510 642 4995.
E-mail address: Lglass@berkeley.edu (N.L. Glass).
[1] Authors contributed equally to this work.
[2] Present address: 9500 Gilman Dr. Muir Biology Rm 5135, La Jolla, CA 92093-0116, United States.

1087-1845/$ - see front matter © 2010 Published by Elsevier Inc.
doi:10.1016/j.fgb.2010.06.010

evaluate whether mutations in the *FAR8* and *FAR9/10* homologs in *N. crassa*, termed *ham-3* and *ham-4* respectively cause a similar cell fusion phenotype to that observed in *ham-2* mutants. We show that *ham-2*, *3* and *4* mutants share a similar vegetative fusion defect, but undergo sexual cell fusion. However, the *ham* mutants show an abnormal meiosis phenotype as well as aberrant ascospore development. The phenotypic similarities between *ham-2*, *3* and *4* mutants suggest they are in the same pathway and regulate diverse cellular processes during both vegetative growth and sexual reproduction in *N. crassa*.

2. Materials and methods

2.1. Strains, growth media and conditions

The strains used in this study are listed in Table 1. Strains were grown on Vogel's minimal medium (Vogel, 1956) with required supplements. BDES medium was used to induce colonial growth (Brockman and de Serres, 1963). Crosses were performed on Westergaards's medium (Westergaard and Mitchell, 1947). The *ham-4* (NCU00528; *Δham-4*) deletion strains, the *ham-3* (NCU08741; *Δham-3*) deletion strains, and the *ham-2* (NCU03727; *Δham-2*) deletion strain (Table 1) were obtained from The Fungal Genetics Stock Center (FGSC) (Colot et al., 2006; McCluskey, 2003). The strain FGSC 4564 was used as a helper for crosses when the female could not produce sexual structures (Perkins, 1984). Growth rates were assessed using the race tube method (Ryan et al., 1943). Electroporation was performed according to (Margolin et al., 1997) with 1.5 kV setting.

2.2. Nucleic acid techniques

Genomic DNA was isolated as described (Lee et al., 1988). Southern hybridization was performed as described (Sambrook and Russell, 2001). Sequencing was performed by the Berkeley DNA sequencing facility (http://mcb.berkeley.edu/barker/dnaseq). Oligonucleotides were obtained from MWG Biotech (www.mwg-biotech.com) and IDT (www.idt.com). The following primers were used: YDR200CFOR371 AGCAACAGCAGCCATCATCG, YDR200CREV2193 TTGTATCAACGCACGCTCCTG, vps64-16 FOR TCTAGACATGTTCATCTCGCAAAATCTCTTCAAC, vps64-16 REV TTAATTAAATTCTTCGCCTGCGGCTGCCACC. Taq polymerase (Promega) was used for routine PCR and PfuTurbo (Stratagene) or Phusion (Finnzymes) was used for high fidelity PCR for cloning.

Repeat induced point (RIP) mutation (Selker, 2002), a naturally mutagenic process in *N. crassa* was used to create *ham-4* point mutation mutants. A fragment amplified by oligonucleotides YDR200CFOR371 and YDR200CREV2193 was cloned into pCB1004, and transformed into strain I-1-83 (Table 1). Hygromycin-resistant transformants were crossed to FGSC 988 to obtain RIP mutants. Progeny were screened for sensitivity to hygromycin (to insure loss of the ectopic transformed *ham-4* fragment and retention of the native mutated *ham-4* locus) and morphological defects. Resulting mutant progeny identified by short aerial hyphae (~24%) were screened for restriction length fragment polymorphisms (RFLPs) at the *ham-4* locus (NCU00528) using a PCR product amplified using oligonucleotides *vps64*-16 FOR and *vps64*-16 REV and digested with *Sau3A* (New England Biolabs).

Cassettes were kindly provided by Hildur Colot for knocking out *vps39* (NCU01539). Deletion strains were constructed as previously described (Colot et al., 2006) and Southern blotting was used to confirm correct integration of the *hph* cassette (data not shown).

The striatin domain, WD repeats, and N221 like protein domain were identified according to Pfam (http://pfam.sanger.ac.uk/). Transmembrane sequences were identified using TopPred (http://mobyle.pasteur.fr/cgi-bin/MobylePortal/portal.py) and verified using TMPRED (http://www.ch.embnet.org/software/TMPRED_form.html). Coils (http://www.ch.embnet.org/software/COILS_form.html) and Paircoil2 (http://groups.csail.mit.edu/cb/paircoil2/paircoil2.html) were used to predict coiled-coil domains in the protein sequences. The calmodulin-binding motif was identified using The Calmodulin Target Database (http://calcium.uhnres.utoronto.ca/ctdb/pub_pages/search/search.htm). A caveolin-binding motif was found in the striatin domain of *ham-3*, which is consistent with the sequence of the striatin domain in *F. verticillioides* FSR-1 and *S. macrospora* PRO11 (Shim et al., 2006).

2.3. Quantitative heterokaryon and conidia formation test

A heterokaryon test between mutant strains and a wild-type tester strain was performed to assess hyphal fusion frequency as previously described (Xiang et al., 2002). A conidial suspension of ~10^7 conidia of the heterokaryon tester strain FGSC 4564 was mixed with ~10^3 conidia of the strains CR16-7 (*ham-4*^{RIP1}), CR16-16 (*ham-4*^{RIP3}), AS2-4 (*his-3 ham-3*::*hph*), AS1-40 (*his-3 ham-4*::*hph*), the negative control strain CR1-10 (*ham-2*^{RIP1}) and the wild-type positive control strain I-1-83 or FGSC 6103. The mixed conidial suspensions were plated on BDES minimal media and grown for 6 days. The colonies resulting from fusion events to form a heterokaryon were counted. The amount of viable conidia in each suspension was determined by germinating the conidia on BDES plates containing supplements (adenine and histidine) and counting the number of resulting colonies. This experiment was repeated three times with similar results.

The amount of conidia each strain produced was determined by inoculating conidia into Vogel's MM tubes and allowing strains to grow for 5 days at 25 °C. After 5 days, 1 ml of water was added to the tube and vigorously vortexed (30 s) to release conidia. The conidia were then counted using a hemacytometer. This experiment was repeated three times with similar results.

2.4. Microscopy

Conidial fusion was assessed using 3–5 day old cultures grown in Vogel's MM (Vogel, 1956) tubes at room temperature (~22 °C). One ml of water was added to the tubes and vigorously vortexed. Conidia were filtered through cheesecloth to remove mycelia,

Table 1
Strains used in this study.

Strain	Genotype	Origin
FGSC 988	ORS 8-1 *a*	FGSC
FGSC 2489	74 OR23 *A*	FGSC
FGSC 6103	*his-3 A*	FGSC
FGSC 4564	*ad-3B cyh-1 a*^{ml}	FGSC
FGSC 11299	*ham-3*::*hph A*	FGSC
FGSC 11300	*ham-3*::*hph a*	FGSC
FGSC 12081	*ham-4*::*hph A*	FGSC
FGSC 12080	*ham-4*::*hph a*	FGSC
FGSC 12091	*ham-2*::*hph A*	FGSC
I-1-83	*ad-3A his-3 A*	Gift from A. J. Griffiths
AS2-4	*his-3*; *ham-3*::*hph a*	FGSC 11300 × FGSC 6103
AS1-40	*his-3 ham-4*::*hph A*	FGSC 12080 × FGSC 6103
AS3-1	*his-3*; *ham-2*::*hph a*	FGSC 12091 × FGSC6103
CR16-7	*ad-3A his-3 ham-4*^{RIP1} *a*	FGSC 988 × I-1-83 (*ham-4*^{RIP1})
CR16-8	*ham-4*^{RIP2} *a*	FGSC 988 × I-1-83 (*ham-4*^{RIP2})
CR16-16	*ad-3A his-3 ham-4*^{RIP3} *A*	FGSC 988 × I-1-83 (*ham-4*^{RIP3})
CR1-10	*pyr-4*; *ham-2*^{RIP1} *A*	Xiang et al. (2002)
CR3-17	*ham-2*^{RIP} *A*	Xiang et al. (2002)
CR65-1	*vps39*::*hph A*	*mus-51* (*NCU01539*::*hph*) × FGSC 988
P1-54	*his-3 Sad-1*^{RIP78} *mep A*	Gift from P. Shiu
P1-68	*his-3 Sad-1*^{RIP141} *mep a*	Gift from P. Shiu
R11-03	*H1*::*GFP A*	Gift from D. Jacobson
R12-60	*H1*::*GFP a*	Gift from D. Jacobson

and plated on Vogel's MM solidified with 1.5% agar. An aliquot of 300 μl of 10^7/ml conidia were spread evenly across each plate. The plates were incubated for 4–10 h at 30 °C. Agar slices were removed from the plates, and conidia were examined by differential interference contrast (DIC) microscopy for fusion every 2 h. Micrographs were taken with a Hamamatsu digital C4742-95 CCD camera (Hamamatsu, Japan) using the Openlab software program (Coventry, United Kingdom) and a Zeiss Axioskop II microscope. Fusion was measured by counting conidial germlings touching each other, and fusion pegs or CATs between these germlings. Approximately one hundred cells were counted for each replicate and three independent replicates were performed for each strain. The percent germling fusion for each strain was graphed using Excel (Microsoft). Micrographs taken using a Zeiss dissecting microscope were captured using a Micropublisher 5.0 RTV camera using Q capture image software (Surrey, BC, Canada).

Perithecia were dissected as previously described (Xiang et al., 2002). Trichogyne assays were performed as previously described (Bistis, 1983; Fleissner et al., 2005; Kim and Borkovich, 2004). Briefly, FGSC 988 (WT), FGSC 11300 (*Δham-3*), FGSC 12080 (*Δham-4*) and FGSC 12091 (*Δham-2*) were inoculated onto 2% water agar and incubated for 5 days at room temperature. Blocks of water agar with approximate dimensions 1.0 cm × 1.0 cm × 0.3 cm were placed on top of the protoperithecia. A microconidial suspension of the opposite mating type (FGSC 2489 or H1-GFP (R11-03 and R12-60); Table 1) was inoculated on top of the block followed by a 20 h to 8-day incubation at room temperature. Data from three independent replicates were pooled to determine the percentage of conidia whose nuclei had disappeared as a result of trichogyne fusion. Protoperithecia and trichogynes were observed using a dry 40× objective.

To compare ascospore morphology, ascospores ejected from perithecia from homozygous and heterozygous crosses were collected. Ascospores were suspended in a 10% glycerol and water solution and observed under the microscope with a 40× objective. For each cross, ascospores from three independent replicates were pooled and approximately 100 spores were scored as either normal, abnormal and melanized or white.

Vacuoles were stained with 5,6-carboxy-fluorescein-di-acetate (CFDA). CFDA was diluted from a stock solution of 2 mg/ml in DMSO to 0.2 mg/ml in water and placed onto *N. crassa* strains grown on agar. After a ten-minute incubation, agar slices were placed on glass slides and conidia or hyphae were observed using a standard FITC filter.

2.5. Acriflavine staining

Acriflavine staining of asci resulting from homozygous and heterozygous crosses was performed according to the protocol developed by Raju (1986a). Perithecia were collected at 6–8 days post fertilization and were incubated at 30 °C in 4 N hydrochloric acid for 30 min. The perithecia were then rinsed and incubated at 30 °C in acriflavine for 30 min. The acriflavine was removed and the samples were washed 3 times with an HCl-70% ethanol mixture (2:98 V/V) and then washed three times with water. Squashes of the perithecia were performed and micrographs were taken of the different stages of ascus development using a fluorescence microscope as described above using an EGFP filter (Chroma Technology Corp., Bellows Falls, Vermont, USA).

3. Results

3.1. Identifying ham-3 and ham-4

In a previous study, we identified the *ham-2* gene, which represented the first molecularly characterized gene required for hyphal fusion in filamentous fungi (Xiang et al., 2002), and which shows significant similarity to a protein encoded by *FAR11* in *S. cerevisiae*. Far11 was subsequently shown to be part of a complex that physically interacts with five other proteins: Far3, Far7, Far8, Far9 and Far10 (Kemp and Sprague, 2003). Blastp (Altschul et al., 1997) was used to search the *N. crassa* predicted proteins (http://www.broad.mit.edu/annotation/fungi/neurospora/) for homologs to FAR3, FAR7, FAR8, FAR9 and FAR10. Single homologs in the *N. crassa* genome to *FAR9/10* (NCU00528) and *FAR8* (NCU08741) were identified, but homologs of either *FAR3* or *FAR7* were not recovered (Glass et al., 2004). NCU08741 encodes a predicted protein of 854 aa that shows significant similarity to *S. macrospora* PRO11, *F. verticillioides* FSR-1 and *S. cerevisiae* FAR8. The predicted protein product of NCU08741 showed the conserved domain structure of the striatin family, whose founding member was isolated from rat neurons (Castets et al., 1996), including a calmodulin-binding domain, which is thought to allow striatin proteins to act as Ca^{2+} sensors (Bartoli et al., 1998). The striatin domain of NCU08741 and most striatin-like proteins (including PRO11 and FSR-1), contain a caveolin-binding motif, a calmodulin-binding domain, a coiled-coil domain and WD repeats, which are protein interaction domains (Smith et al., 1999) (Fig. 1A).

We hypothesized that strains containing a deletion of NCU08741 would have a similar phenotype to *ham-2* mutants. Strains containing a deletion of NCU08741 (FGSC 11300; Table 1) grew slowly (~3.5 cm/day as compared to wild-type FGSC 988 at ~7.5 cm/day), had very short aerial hyphae (Fig. 1B, tube 3) and produced ~100 times fewer conidia than the equivalently grown wild-type strain FGSC 988 (data not shown), a phenotype similar to a *ham-2* mutant (Xiang et al., 2002). We refer to NCU08741 as *hyphal anastomosis-3* (*ham-3*) locus to reflect the requirement of this gene for cell fusion (see below).

NCU00528 encodes a predicted 761 aa protein, which showed significant similarity to both Far9 and Far10 (e-19). The NCU00528 protein has a predicted FHA domain at its N-terminus, a coiled-coil domain and a transmembrane domain at the C-terminus (Fig. 1A). FHA domains are regions of ~100 aa that fold into an 11-stranded beta sandwich and have been characterized as phosphopeptide recognition domains found in many diverse regulatory proteins.

Using Repeat Induced Point (RIP) mutation, a naturally mutagenic process in *N. crassa* (Selker, 2002), several mutant alleles of NCU00528 were recovered (CR16-7, CR16-8, and CR16-16; Table 1). NCU00528 was sequenced from CR16-7 and CR16-8; altered codons were S175L, A202T, V205I, P206L, and Q228STOP (CR16-7) and M143I, M163I, G178S, M194I, A203T and W226STOP (CR16-8) (Fig. 1A). The stop codons in the NCU00528 RIP alleles in both CR16-7 and CR16-8 would result in a truncated protein of ~200 amino acid residues and which still retains the N-terminal part of the FHA domain. Strains containing the mutant NCU00528 RIP alleles were characterized by slow growth and a tuft of conidia at the top of a tube (Fig. 1B, tube 5). The growth rate of a representative mutant, CR16-8 was reduced to ~5 cm/day as compared to the wild-type growth rate of ~7.5 cm/day.

We also evaluated the phenotype of a strain containing a deletion of NCU00528 (FGSC 12080; Table 1) to compare to the NCU00528 RIP mutants. The *Δ*NCU00528 strain grew more slowly than CR16-8 (only ~4 cm/day), but was otherwise phenotypically similar to the NCU00528 RIP mutants (short aerial hyphae and a characteristic tuft of conidia (Fig. 1B, tube 4). Also, similar to the *ham-2* mutant (Xiang et al., 2002), the *Δ*NCU00528 strain produced ~100 times fewer conidia than a wild-type strain (data not shown). Most importantly for this study, the strain containing a deletion of NCU00528 was also a hyphal fusion mutant (see below). We therefore refer to NCU00528 as the *hyphal anastomosis-4* (*ham-4*) locus.

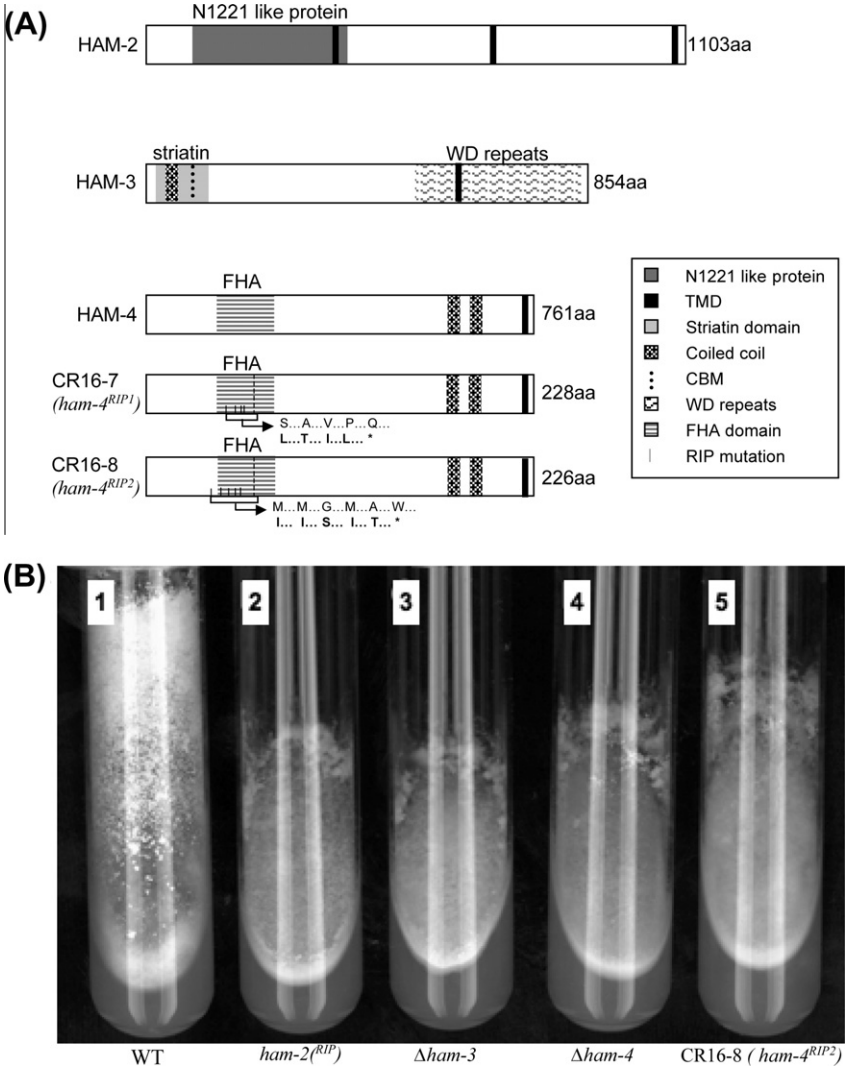

Fig. 1. A. Domain structure of HAM-2, 3, and 4. The altered amino acid residues of CR16-7 (*ham-4*^{RIP1}) and CR16-8 (*ham-4*^{RIP2}) are depicted with black dashes and the location of the new stop codon is a vertical dashed line. The original amino acids that were altered are written in gray and the resulting amino acids after RIP are written in black with an asterisk representing a stop codon. TMD – transmembrane domain, CBM – calmodulin-binding motif, FHA – forkhead-associated domain, B. The macroscopic morphology of the *Δham-3* and *Δham-4* strains is similar to *ham-2* mutants. (1) FGSC 988 (WT) grown in a slant tube has typical extensive aerial hyphae and conidiation. (2) CR3-17 (*ham-2*^{RIP}) has short aerial hyphae and makes a tuft of conidia at the top of the slant tube. (3) FGSC 11300 (*Δham-3*) has a similar macroscopic phenotype. (4) FGSC 12080 (*Δham-4*). (5) CR16-8 (*ham-4*^{RIP2}) also makes a tuft of conidia at the top of the slant tube.

3.2. Quantifying cell fusion in the Δham-2, Δham-3, and Δham-4 mutants

The previously characterized *ham-2* mutant has a severe homotypic fusion defect (Xiang et al., 2002). We therefore used a quantitative conidial fusion assay (Pandey et al., 2004) to assess the ability of the *ham-3* and *ham-4* mutant strains to undergo homotypic fusion. Homotypic fusion is defined as fusion between strains of identical genotype where as heterotypic fusion is between strains of different genotypes. Fig. 2 shows the comparative ability of *Δham-3*, *Δham-4*, *ham-4*^{RIP2} and WT conidial germlings to fuse between themselves over a time course from 4–10 h post-inoculation. The wild-type strain FGSC 988 showed a robust ability to undergo fusion (Fig. 2A). A representative micrograph of wild-type germling fusion at the four hour time point is shown in Fig. 2B (note the interconnected nature of the conidial germlings). In contrast to WT, *Δham-3*, *Δham-4* and the *ham-4*^{RIP2} mutant (CR16-8) showed a significantly reduced ability to undergo fusion. However, in contrast to the *Δham-4* strain, the *ham-4*^{RIP2} mutant displayed ability to undergo self-fusion, especially at later time points. Thus, this mutation in *ham-4* (which retains much of the FHA domain) may represent a partial loss-of-function allele, consistent with its less severe self-fusion defect (Fig. 2A). The morphology of the germinating conidia in the *ham* mutants was strikingly different from that of WT germlings and similar to each other (Fig. 2B). The germ tubes of *ham* mutant strains grew away from the inoculation point, while in WT the germ tubes of germlings grew towards each other and ultimately underwent fusion. This germination phenotype is similar to what has been reported for *ham-2* mutants (Roca et al., 2005).

The conidial germling fusion assay tested the ability of strains to undergo homotypic fusion, but did not provide information about whether wild-type strains can respond to, and fuse with, *Δham-3*, *Δham-4* or *ham-4*^{RIP} strains. Using a quantitative heterokaryon assay, it was previously shown that strains containing mutations in *ham-2* have a 1000-fold reduction in the ability to fuse with a wild-type strain (Xiang et al., 2002). In this assay, conidia from the mutant strain and a wild-type fusion competent strain (FGSC 4564; Table 1), containing different auxotrophic markers, are mixed and plated on minimal media. Only those

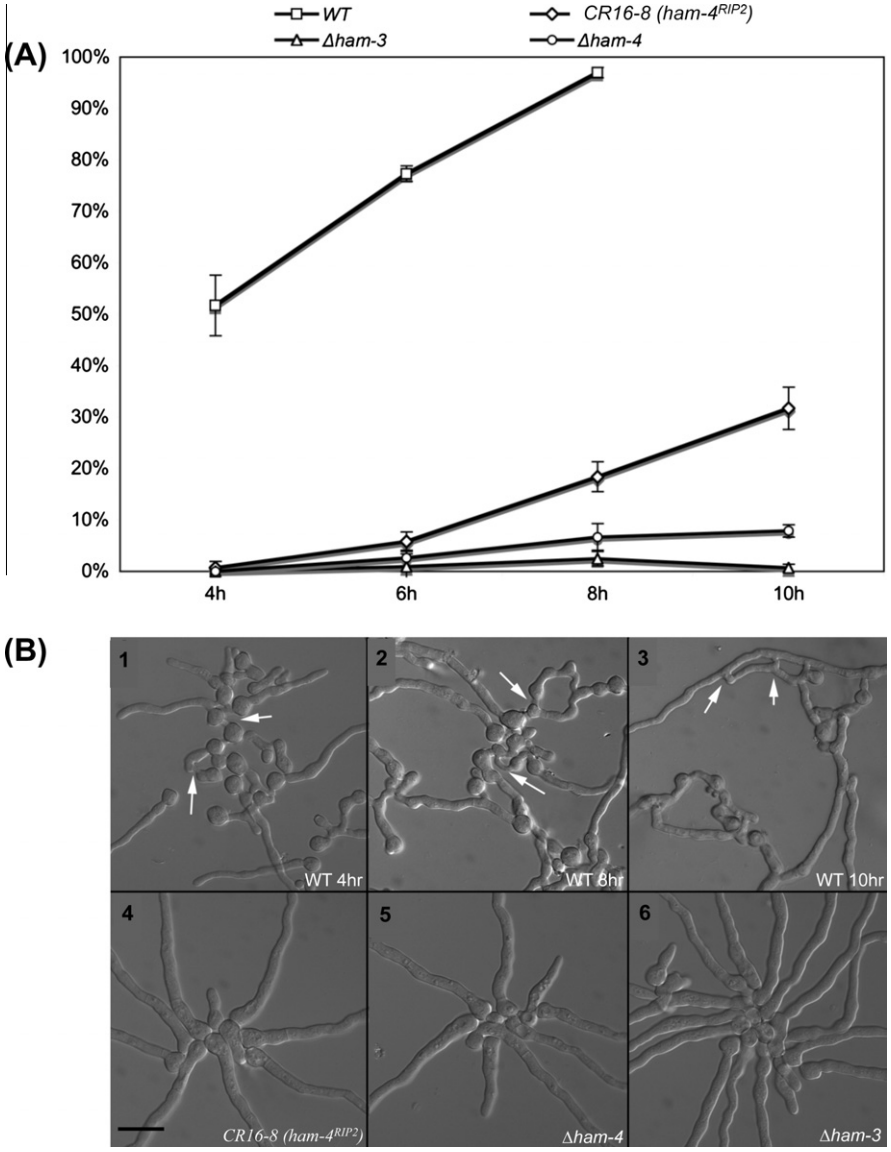

Fig. 2. Germling fusion in *ham* mutants. A. Graph of germling fusion frequency. An aliquot of 300 μl of 10^7/ml conidia was inoculated onto Vogel's MM for 4–10 h. Fusion rates were measured by counting the number of fused cells in the total number of cells (see white arrows in 2B for examples). All samples had >90% germination except FGSC 12080 (*Δham-4*) at 4 h (89%), and FGSC 11300 (*Δham-3*) at 4 h (82%). Fusion in FGSC 988 (WT) could not be measured at 10 h because of over growth. B. Representative morphology of germlings. (1) FGSC 988 (WT) grown for 4 h shows fusion. (2) FGSC 988 (WT) at 6 h. (3) FGSC 988 (WT) at 8 h. Examples of fusion indicated by arrows. (4) CR16-8 (*ham-4*$^{RIP-2}$) at 8 h. Typically, conidial germlings touch each other, but rarely fuse. (5) FGSC 12080 (*Δham-4*) at 8 h. Conidial germlings rarely fuse. (6) FGSC 11300 (*Δham-3*) at 8 h. Conidial germlings rarely fuse and look similar in both *ham-4* mutants tested. Bar = 60 μm.

germlings/hyphae that have undergone fusion with FGSC 4564 and containing the complementary auxotrophic markers, are able to grow on minimal media without additional supplements (heterokaryon test). Similar to strains containing a mutation in *ham-2*, both the *Δham-4* (AS1-40) and the *Δham-3* (AS2-4) deletion strains showed a severe heterotypic fusion defect, with no heterokaryotic colonies recovered (Table 2). By contrast, strains containing the point mutations in *ham-4* (CR16-7; *ham-4*^{RIP1} and CR16-16; *ham-4*^{RIP3}) formed heterokaryons with the wild-type tester strain (FGSC 4564) at a similar frequency to the wild-type control (Table 2). These data suggest that *ham-4*^{RIP} alleles that encode a truncated HAM-4 protein containing only the FHA domain are sufficient for both homotypic and heterotypic fusion.

3.3. Vacuolar morphology of ham-2, ham-3 and ham-4 mutants

In a functional genomics study in *S. cerevisiae*, the *ham-2* homolog *ynl127w* (*FAR11*) and *ham-4* homolog, *vps64* (*FAR 9*) were identified as vacuolar protein sorting (*vps*) mutants due to their improper CPY secretion (Bonangelino et al., 2002). We therefore tested potential *vps* defects of the *ham* mutants in *N. crassa* by observing vacuolar morphology. A *vps* positive control strain containing a deletion of *vps-39* (*vps-39*::*hph* (*Δvps-39*)) was constructed (see Section 2) (Table 1). Vps39 (also known as Vam6) is the guanine nucleotide exchange factor for the Rab GTPase Ypt7, and is required for vacuole fusion and organization (Wurmser et al., 2000). In both *S. cerevisiae* and *Aspergillus nidulans*, *vps39*/*vam6*/*avaB* mutants have defective vacuolar morphology, including small and fragmented vacuoles (Bonangelino et al., 2002; Oka et al., 2004; Raymond et al., 1992). We stained germlings from the *ham* mutants and the *Δvps-39* strain using 5,6-carboxy-fluorescein di-acetate (CFDA), a fluorescent probe that specifically labels vacuoles. While germlings in the *Δvps-39* strain (CR65-1) had tubular and small vacuoles, as expected (Fig. 3), the relative size of vacuoles in all of the *ham* mutants were consistently larger than the wild-type strain FGSC 988 (Fig. 3C–F). The relatively large

Table 2
Frequency of heterokaryon formation in *ham* mutants versus wild type.

Strain	Viable conidia	Heterokaryotic colonies	Percent heterokaryon formation
FGSC6103 (WT)	570 ± 53*	104 ± 2	18.3 ± 2**
CR16-07 (*ham-4^{RIP1}*)	810 ± 81	123.7 ± 10	15.3 ± 2
CR16-16 (*ham-4^{RIP3}*)	590 ± 52	108.7 ± 7	18.4 ± 2
AS1-40 (*his-3 ham-4::hph A*)	496 ± 24	0	0
AS2-4 (*his-3*; *ham-3::hph a*)	553 ± 129	0	0
CR1-10 (*pyr-4*; *ham-2^{RIP1}*)	652 ± 45	0	0
FGSC 4564	4.26×10^6 ± 9	NA	NA

* Standard error is shown for experiments done in triplicate.
** Percent fusion error was calculated using Gaussian error propagation.

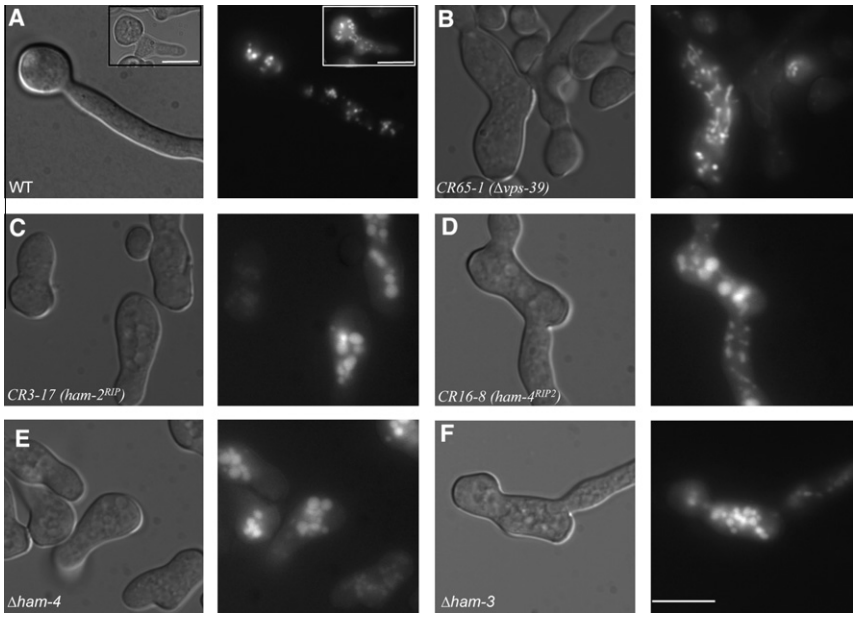

Fig. 3. Vacuolar staining of *ham-2*, *Δham-3*, *Δham-4*, *and ham-4^{RIP2}* germlings. Comparative vacuolar morphology of conidia grown for 4 h at 30 °C and stained with (0.2 mg/ml) 5,6 carboxy fluorescein di-acetate (CFDA). Left panels are DIC micrographs and right panels are the fluorescent micrographs of the same samples. All samples are the same relative size, with the scale bar = 10 μm. (A) FGSC 988 (WT) has small regularly sized vacuoles. (B) CR65-1 (*vps-39::hph*) positive control strain for vacuolar protein sorting has small, tubular vacuoles. (C) CR3-17 (*ham-2*). (D) CR16-8 (*ham-4^{RIP2}*). (E) FGSC 12080 (*Δham-4*). (F) FGSC 11300 (*Δham-3*). *ham* mutants have larger vacuoles.

vacuoles seen in the *ham* mutants were also seen at later time points when the relative growth of germinating spores from the *ham* mutants was equivalent to the wild-type strain (data not shown). Fragmented as well as large vacuoles have been associated with protein sorting defects in *S. cerevisiae* (Raymond et al., 1992).

3.4. The *Δham-2*, *Δham-3* and *Δham-4* mutants show delayed formation of protoperithecia

In addition to germling and hyphal fusion, which occur during vegetative growth, cell fusion is also required during mating in *N. crassa*. Upon nitrogen starvation, a strain of either mating type will produce female reproductive structures termed protoperithecia. Specialized hyphae called trichogynes grow out of the protoperithecia and chemotropic interactions between trichogynes and conidia of opposite mating type ultimately result in cell fusion between the two (Bistis, 1981, 1983). After cell fusion occurs, one or more nuclei from the conidium subsequently travels down the trichogyne and into the protoperithecium. After approximately 4 days, fertile ascogenous hyphae can be observed within the developing perithecium. A second cell fusion event is associated with crozier development and ascus formation (where karyogamy and meiosis occur) (Davis, 2000; Raju, 1992).

Previous results suggested that hyphal fusion is required for formation of protoperithecia in *N. crassa* (Maerz et al., 2008; Xiang et al., 2002). For example, RIP mutations in *ham-2* resulted in a strain that failed to make protoperithecia (Xiang et al., 2002), a phenotype that could be complemented in a heterokaryon with a wild-type strain. We therefore evaluated whether strains containing a deletion of *ham-2*, *ham-3* or *ham-4* were capable of forming female reproductive structures. To our surprise, strains containing a full deletion of *ham-2* (*Δham-2*, FGSC 12091) formed wild-type looking protoperithecia, although at a later time point than that observed for a wild-type strain (FGSC 988) (Table 3). Similarly, *Δham-3* and *Δham-4* strains produced normal looking protoperithecia, but were 1–2 days delayed in protoperithecium formation, possibly as a consequence of their slow growth rate. These data indicate that hyphal fusion is not required for the development of morphologically normal female reproductive structures.

3.5. The ham mutants show chemotropic interactions during mating and undergo mating-cell fusion

The *ham-2*, *ham-3* and *ham-4* mutants failed to show chemotropic interactions during germling fusion and are fusion defective (Fig. 2 and Table 2). Thus, we evaluated whether *Δham-2*, *Δham-3*, and *Δham-4* mutants were also affected in mating-cell chemotropic interactions or fertilization by performing a trichogyne-conidium mating assays. All three *ham* strains were delayed in protoperithecial and trichogyne production as compared to a

Table 3
Summary of crosses.

	Male parent						
		× WT		× *Sad-1*		× *Δham* homozygous	
Female parent	Protoperithecia	Perithecia	Ascospores	Perithecia	Ascospores	Perithecia	Ascospores
WT (FGSC 2489)	+	+	+	+	+	ND	ND
Δham-2	+[a]	–	–	–	–	–	–
Δham-3	+[a]	–	–	–	–	–	–
Δham-4	+[a]	+	+[b]	+	+	+	+[b]
FGSC 6103 + a^{m1}	+	+	+	+	+	ND	ND
Δham-2 + a^{m1}	+	+	+[b]	+	+	+	+[b]
Δham-3 + a^{m1}	+	+	+[b]	+	+	+	–
Δham-4 + a^{m1}	+	+	+[b]	+	+	+	+[b]

[a] Delayed.
[b] Abnormal ascospores.

wild-type strain (FGSC 988). Wild-type trichogynes reached microconidia within 40 h, while *Δham-3* and *Δham-4* trichogynes took 7 days to reach microconidia of the opposite mating type. Despite severely reduced growth rate of trichogynes towards microconidia, the *Δham-3* and *Δham-4* trichogynes were attracted to and wrapped around microconidia of the opposite mating type in a manner indistinguishable from wild-type strain FGSC 988 (Fig. 4A). Unlike the results using the *Δham-3* and *Δham-4* mutants, trichogyne assays with the *Δham-2* mutant were inconclusive. Trichogynes were observed growing from protoperithecia through the agar block toward microconidia on top of the block. However, after 8–9 days, the *Δham-2* trichogynes still had not reached the microconidia. Vegetative hyphae began growing over the agar blocks, making imaging of trichogyne-conidium interactions impossible.

We then evaluated whether mating-cell fusion was affected in the *Δham-3* and *Δham-4* mutants. We used microconidia from strains containing a histone-1-GFP (H1-GFP) construct (R19-22; Table 1 (Freitag et al., 2004)) to determine whether nuclei traveled from the microconidium to the trichogyne as a consequence of trichogyne-conidium fusion. When trichogynes of wild-type strain FGSC 2489 wrapped around nuclear H1-GFP labeled microconidia of the opposite mating type (R12-60), 87% of nuclei disappeared, indicating mating-cell fusion had occurred (Fig. 4D). Of the *Δham-3* trichogynes that circled around wild-type H1-GFP microconidia, 52% (n = 33) underwent mating-cell fusion, as assessed by loss of nuclear H1-GFP fluorescence in the microconidia. In *Δham-4*, 59% (n = 149) of the trichogynes that circled around wild-type H1-GFP labeled microconidia underwent mating-cell fusion. These data show that although there is a reduction in both the speed and number of successful mating-cell fusions, *Δham-4* and *Δham-3* mutants are capable of both sexual chemotropic interactions and sexual cell fusion, which results in nuclear migration through the trichogyne.

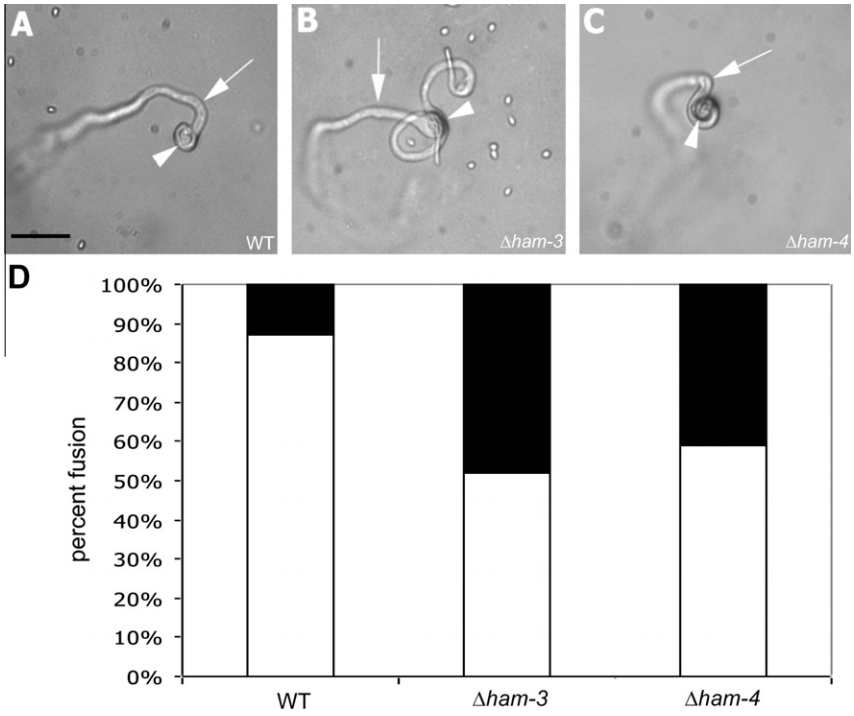

Fig. 4. *Δham-3* and *Δham-4* both undergo trichogyne-conidium fusion but are delayed in trichogyne development compared to wild-type. (A) Wild type (FGSC 2489) trichogyne (arrow) approaches and circles a conidium of the opposite mating type, indicated by an arrowhead, after 16 h of incubation. (B) *Δham-3 A* (FGSC 11299) trichogyne wraps around a conidium of the opposite mating type after 3 days of incubation. (C) *Δham-4 A* (FGSC 12081) trichogyne wraps around a conidium after 2 days of incubation. (D) Percentage of nuclei from a H1::GFP conidium that were transported into the trichogyne as a result of fertilization. Wild-type fusion was measured over 40 h, n = 67, *Δham-3* was measured over 7 days, n = 33, and *Δham-4* was measured over 7 days n = 149. Bar = 15 μm.

3.6. The Δham-2 and Δham-3 mutants are blocked in female sexual development following fertilization

To test their ability to complete a mating cross as a female, *Δham-2*, *Δham-3* and *Δham-4* strains were grown on mating plates until they produced protoperithecia and then were crossed using *Sad-1* as a male (Fig. 5). *Sad-1* mutants suppress meiotic gene silencing of unpaired DNA (MSUD) (Shiu et al., 2001) and therefore eliminate silencing from affecting sexual development. The *Δham-4* crosses with *Sad-1* resulted in production of mature sexual structures (perithecia). Perithecia from the *Δham-4* × *Sad-1* crosses were indistinguishable from those of a wild-type cross and contained viable ascospores (Table 3), although the density of perithecia on mating plates was less than wild type (data not shown). In contrast, perithecia in *Δham-2* and *Δham-3* crosses with *Sad-1* failed to develop and remained immature (Fig. 5; Table 3). No sexual tissue (paraphyses, ascogenous hyphae, croziers or asci) were observed in these crosses. These results suggest a post-mating defect in *ham-3* mutants because trichogyne-conidium fusions were observed in *ham-3* crosses.

Crosses between *Sad-1* strains as a female (P1-54 *A* or P1-68 *a*; Table 1) and *Δham-2*, *Δham-3* or *Δham-4* strains as a male were fully fertile. The crosses resulted in wild-type looking perithecia, in which wild-type ascospores developed (Fig. 6). These data indicate that *ham-2* and *ham-3* mutants have a sexual defect that is female autonomous in development of perithecia. To test this hypothesis, we created heterokaryons of *Δham-2*, *Δham-3* and *Δham-4* with a helper strain a^{m1} (FGSC 4564). The a^{m1} mutant contains a mutation at the *mating type* locus such that this mutant still makes female reproductive structures, but cannot participate in a cross as either a female or male; a^{m1} nuclei are not active in ascogenous hyphae (Perkins, 1984; Raju, 1992). Heterokaryons between *Δham-2*, *Δham-3* or *Δham-4* and the helper strain (*Δham-2* + a^{m1}); (*Δham-3* + a^{m1}); (*Δham-4* + a^{m1}) were fertile as females when crossed to a *Sad-1* or wild-type strain FGSC 2489 (Table 3). These data indicate that *ham-2* and *ham-3* mutants have a defect in female sexual development following fertilization, but before ascogenous hyphae development.

3.7. Δham-2, Δham-3 and Δham-4 mutants show abnormal meiosis and ascospore development

When *Δham-2*, *Δham-3*, and *Δham-4* strains were used as males in a cross with a wild-type female instead of a *Sad-1* female, we observed an unexpected phenotype. The ascospores from these crosses had unusual sizes and shapes (Fig. 7). These data indicated that MSUD silenced the unpaired *ham* genes in these crosses, suggesting that homozygous crosses between *ham* mutants would show similar ascospore defects. We therefore used the (*his-3*; *ham-2*::*hph* *a* + a^{m1}) heterokaryon as a female and crossed it to

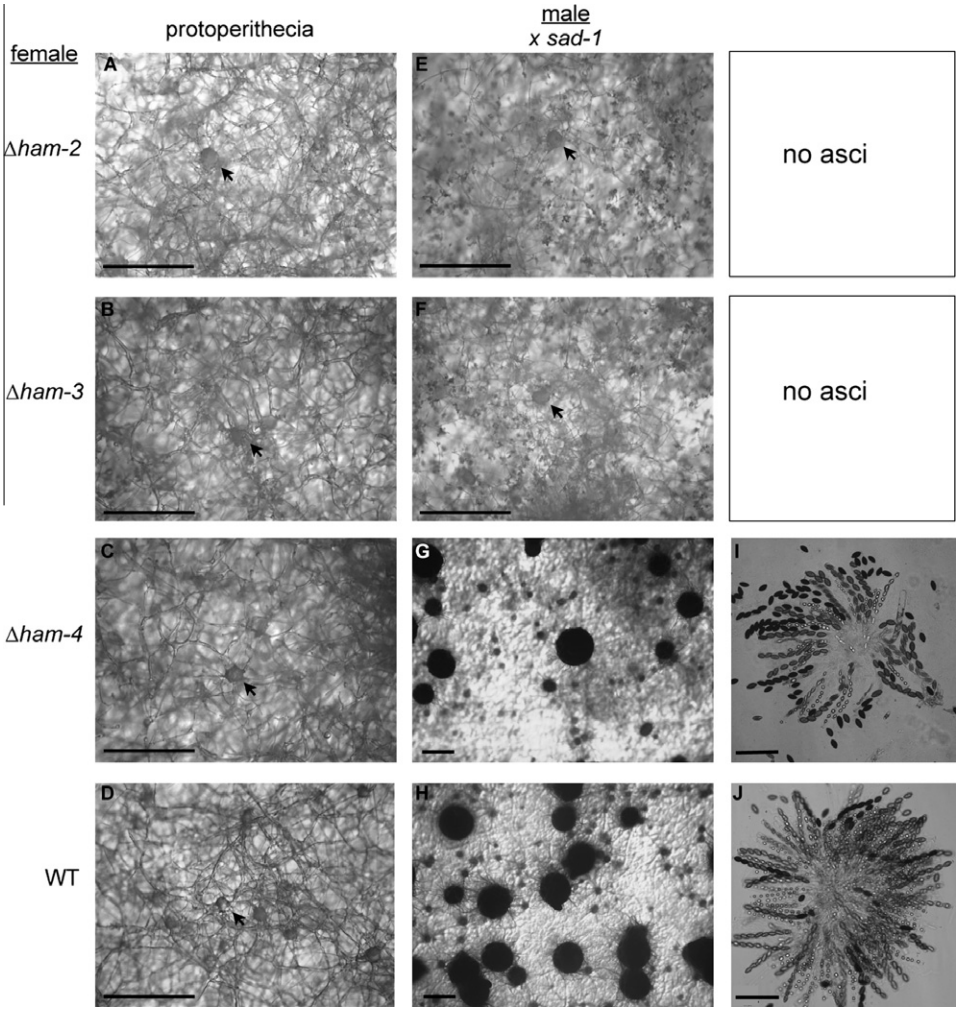

Fig. 5. *Δham-2*, *Δham-3*, and *Δham-4* used as females crossed with *Sad-1* strains of the opposite mating type. Protoperithecial development (indicated by arrows) in: (A) *Δham-2*, (B) *Δham-3*, (C) *Δham-4* and (D) wild type (FGSC 2489). (E–H) were taken 13 days post fertilization. Perithecia resulted from the (G) *Δham-4* × *Sad-1* and (H) FGSC 6103 × *Sad-1* crosses. Squashes from the resulting perithecia were (I) *Δham-4* × *Sad-1*, (J) FGSC 6103 × *Sad-1*. The *Δham-2* and *Δham-3* crosses lacked any sexual tissue, including paraphyses, ascogenous hyphae and asci. Scale bars for A–H are 0.5 mm. Scale bar for squashes (I and J) equals 130 μm.

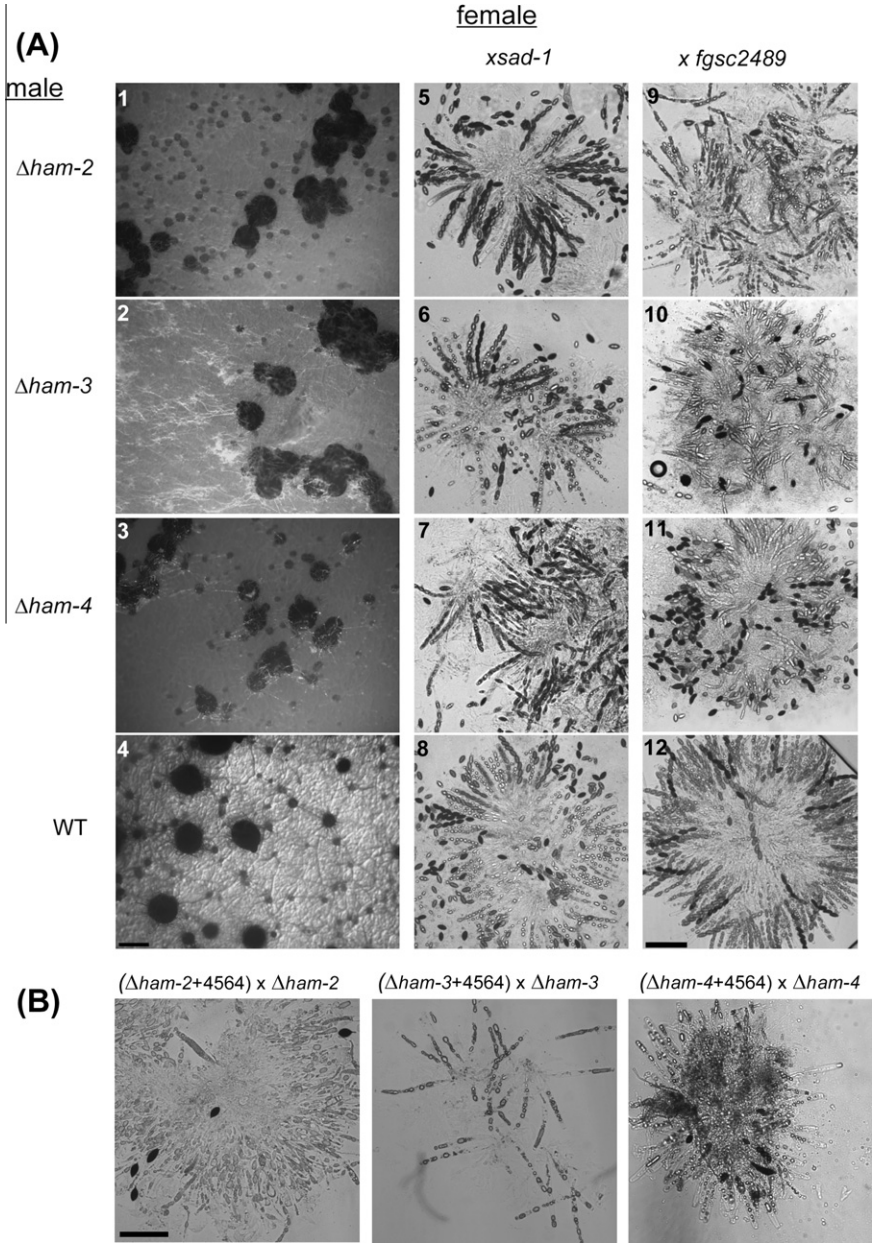

Fig. 6. *Δham-2*, *Δham-3* and *Δham-4* crosses when used as males and crossed with either *Sad-1* or a wild-type strain of the opposite mating type. (A) Perithecia developed when *Sad-1* was crossed with: (1) *Δham-2*, (2) *Δham-3*, (3) *Δham-4* and (4) wild type. Panels 5–8, respectively, are rosettes recovered from these crosses. Panel 9 is a rosette recovered from wild type crossed with *Δham-2*, panel 10 is a rosette resulting from wild type crossed with *Δham-3* and panel 11 is a rosette from wild type crossed with *Δham-4*. Scale bar for panels 1–4 equals 0.5 mm. The scale bars for 5–12 represent approximately 130 μm. (B) Squashes from homozygous crosses: (1) (*Δham-2* + FGSC 4564) × *Δham-2*); (2) (*Δham-3* + FGSC 4564) × *Δham-3*) and (3) (*Δham-4* + FGSC 4564) × *Δham-4*). The scale bars for 1–3 represent 130 μm.

Δham-2 A. As predicted, the resulting perithecia contained a reduced number of ascospores per rossette (Fig. 6B) and 93.5% ($n = 91$) of these spores were abnormal (Fig. 7), deviating either from the typical elliptical shape and/or the typical spore size. Similarly, *ham-3* homozygous crosses ((*his-3*; *ham-3*::*hph a* + a^{m1}) × *ham-3*::*hph A*) resulted in a severe decrease in ascospore production (Fig. 6B); ascospores from this cross were never ejected and we were unable to recover enough spores to analyze. By contrast, *ham-4* homozygous crosses ((*his-3*; *ham-4*::*hph A* + a^{m1}) × *ham-4*::*hph a*) (Fig. 6B) showed a much less severe ascospore phenotype. Only 64.5% ($n = 124$) of the ascospores were abnormal, although the number of ascospores per rosette was similar to that of wild type (Fig. 7).

Heterozygous crosses, using the *ham-2*, *3*, *or 4* + a^{m1} heterokaryons as female and crossed with a wild type male strain, showed a slightly less severe ascospore phenotype as compared to the homozygous crosses (Fig. 7B). Most notably ((*ham-3*::*hph* + a^{m1}) × WT) crosses resulted in ascospores (Fig. 7A), whereas *ham-3* homozygous crosses were completely sterile. The ascospore phenotypes of the (*Δham-2*, *3*, or *4* + a^{m1}) × WT crosses were completely suppressed when the *Sad-1* strain was used as a male, with all three crosses resulting in only ~4–7% abnormal ascospores, a value comparable to a wild-type cross with *Sad-1* ((FGSC 6103 + a^{m1}) × *Sad-1*; 3.0% ($n = 100$) abnormal ascospores).

3.8. Nuclear staining in developing asci

Mutants showing abnormal or delayed meiosis often result in wide range of ascospore phenotypes including barren asci, incorrect spore delimitation, abnormal spore size and shape, and a

decreased number of spores per ascus (reviewed in Raju (1992)). In order to determine if a defect in meiosis occurs in the *ham* mutants, we used acriflavine to stain nuclei at different stages of developing asci from *ham* homozygous crosses (Raju, 1986a). Normal ascus development after crozier formation includes karyogamy (one nucleus), meiosis I (two nuclei), meiosis II (four nuclei), mitosis I (eight nuclei), spore delimitation and mitosis II (two nuclei per ascospore) (Raju, 1980). A number of further mitoses then occur within the delimited ascospores, resulting in up to 32 or more nuclei in mature ascospores. All stages of meiosis and mitosis can be seen in Fig. 8 during the development of a wild type ascus from a ((FGSC 6103 + a^{m1}) × *Sad-1*) cross. In homozygous crosses with *ham-2* ((*his-3*; *ham-2*::*hph a* + a^{m1}) × *ham-2*::*hph A*), *ham-3* ((*his-3*; *ham-3*::*hph a* + a^{m1}) × *ham-3*::*hph A*), and *ham-4* ((*his-3 ham-4*::*hph A* + a^{m1}) × *ham-4*::*hph a*), many asci containing a single nucleus were found in developing perithecia (Fig. 8). These observations indicate successful crozier formation resulting in karyogamy. However, the *ham* homozygous crosses appeared to be delayed in meiosis I as compared to a wild-type cross. This is particularly evident in *ham-2* and *ham-3* homozygous crosses, where a single nucleus was observed in an ascus that would usually contain two or four nuclei in a wild-type cross. By contrast, asci with two nuclei were eventually observed in all the *ham* homozygous crosses. A meiotic malfunction is even more evident during meiosis II and mitosis I in asci of the homozygous *ham* crosses, where spore delimitation occurred, but where fewer than eight nuclei were present in the ascus (Fig. 8B–D). This results in a variable number of large ascospores within one ascus and aborted ascospores lacking nuclei. Heterozygous crosses between the *ham* mutants and wild type ((*ham* mutant + a^{m1}) × WT) also often exhibited aberrant meiosis resulting in asci with various numbers of large ascospores (Fig. 6A). In contrast, the *ham-4* homozygous and heterozygous crosses often proceeded in the correct developmental order and resulted in eight-spored asci, although many of the spores were abnormally shaped. The phenotype of abnormal meiosis and ascospore development was present in all *ham* mutant homozygous crosses.

Ascospores produced from the *ham* homozygous and heterozygous crosses showed a variety of shapes and sizes but often had an extra appendage or tail (Fig. 7). In addition, the cell wall and/or the ability to maintain a correct osmotic potential is compromised such that when the ascospores are suspended in water they burst.

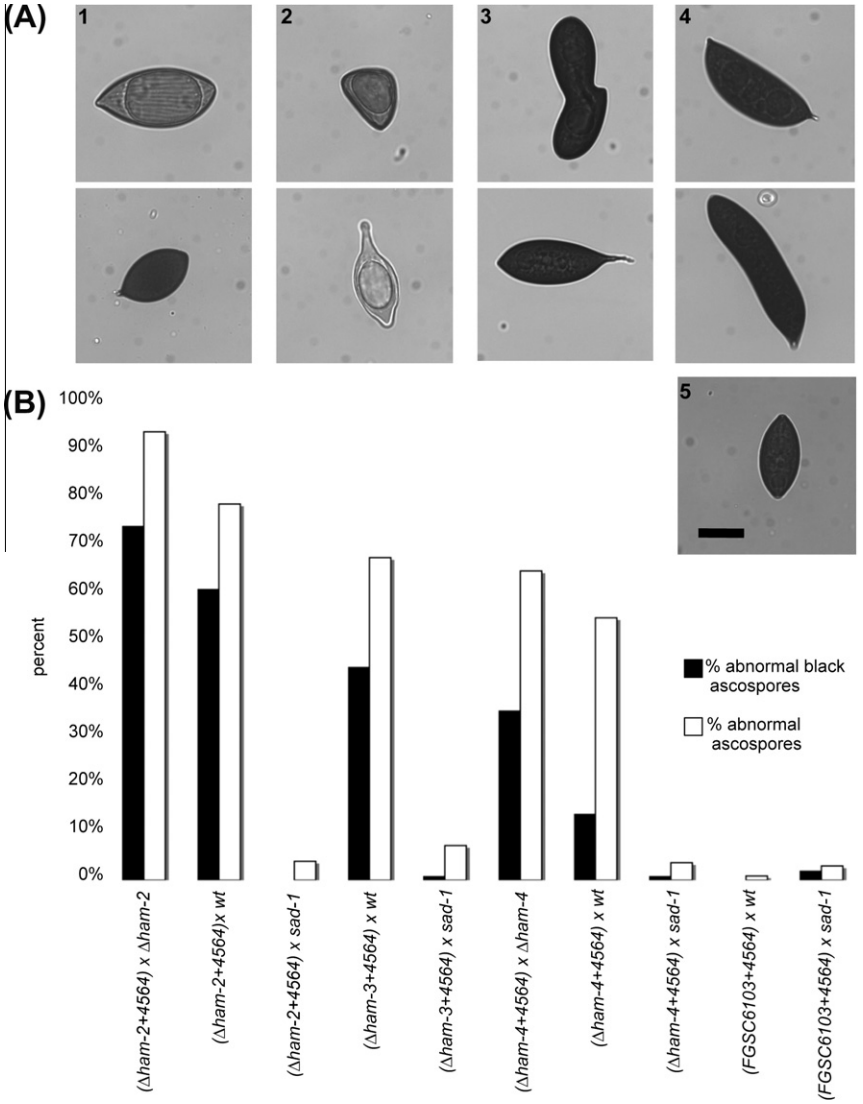

Fig. 7. Examples of ascospores recovered from crosses. (A) (1) (*Δham-4* + FGSC 4564) × FGSC 2489; (2) (*Δham-4* + FGSC 4564) × *Δham-4*; (3) (*Δham-3* + FGSC 4564) × FGSC 2489 and (4) (*Δham-2* + FGSC 4564) × *Δham-2*. (5) A wild type ascospore from an (FGSC 6103 + FGSC 4564) × *Sad-1* cross. Scale bar equals 15 μm. (B). Graph showing the percentage of abnormal ascospores (white bars) collected after ejection from perithecia and percentage of abnormal ascospores that are melanized (black bars).

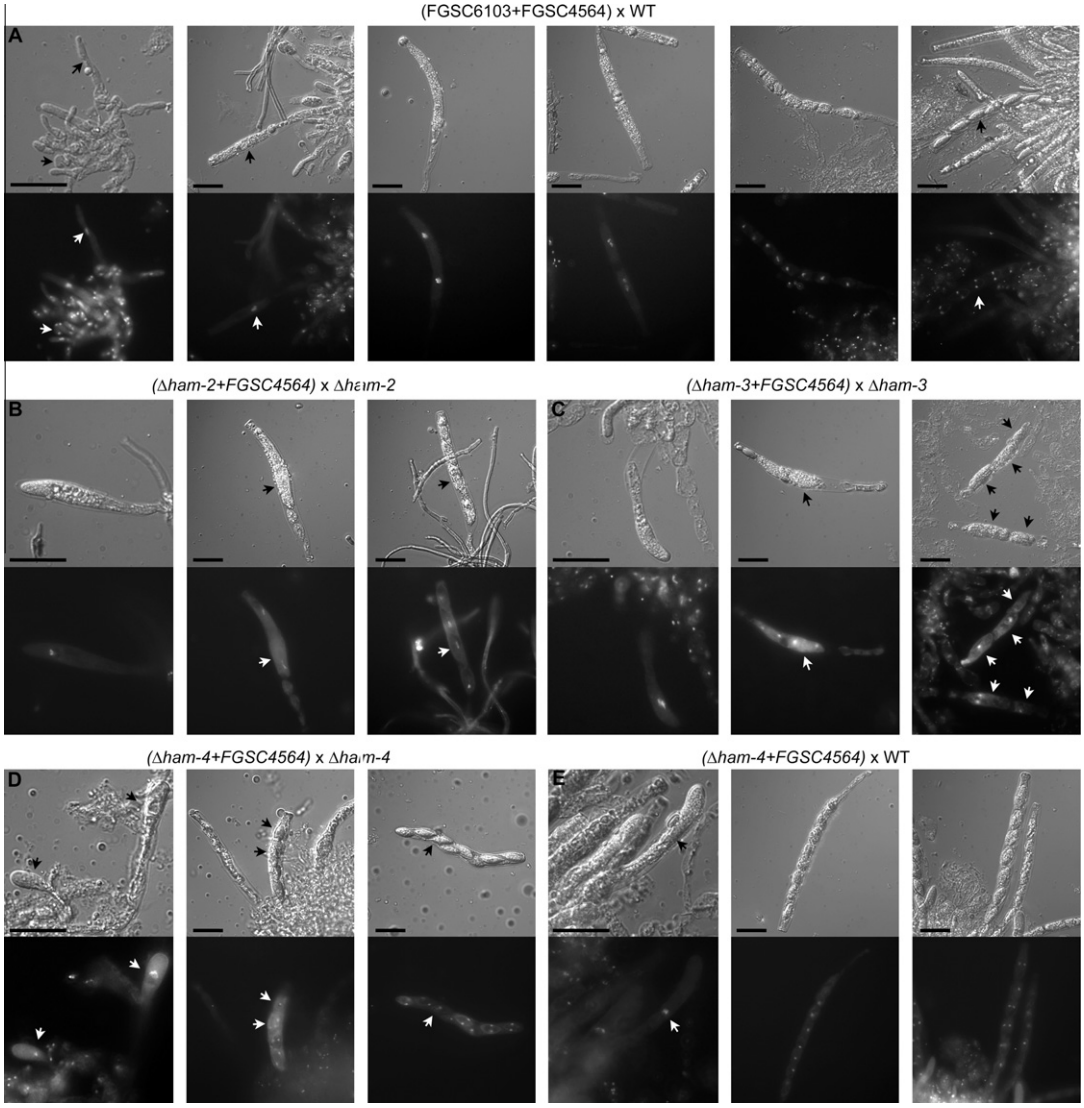

Fig. 8. Acriflavine staining of the nuclei in developing asci. (A) Stages of ascus development from (FGSC 6103 + FGSC 4564) × *Sad-1*, first panel shows a rosette with croziers and early asci indicated with arrows. The second panel shows a diploid nucleus in prophase (arrow), the third panel shows two nuclei after meiosis I, the fourth panel shows four nuclei after meiosis II, the fifth panel shows eight nuclei after the first mitotic division and the sixth panel shows spore delimitation and a second mitotic division resulting in two nuclei per ascospore (arrow). (B) (*Δham-2* + FGSC 4564) × *Δham-2* shows normal karyogamy (first panel) but results in abnormal subsequent meiotic and mitotic divisions as well as spore delimitation. The second panel shows the beginning of spore delimitation (arrow) but only two nuclei in the ascus, and the third panel shows only four large spores already delimited within the ascus containing one nucleus each (example indicated by arrow). (C) (*Δham-3* + FGSC 4564) × *Δham-3* the first panel shows normal karyogamy, the second panel shows spore formation (arrows) with only four nuclei in the ascus, and the third panel depicts asci with incorrect numbers of ascospores that are large and have abnormal morphologies (arrows). (D) (*Δham-4* + FGSC 4564) × *Δham-4* the first panel shows normal karyogamy, panel two shows abnormal spore delimitation, and panel three shows an ascus with eight ascospores that have aberrant morphologies and orientations (arrow points to an ascospore with a tail). (E) (*Δham-4* + FGSC 4564) × R15-7 shows that some asci that develop normally from this cross. Scale bar represents 30 μm.

This phenomenon is alleviated when the spores are suspended in 5% FIGS or in a 10% glycerol solution. As with wild type crosses, heat shock was required for ascospore germination, and many of the ascospores germinated despite their abnormalities (data not shown).

4. Discussion

Based on human and *S. cerevisiae* data, we interrogated the *N. crassa* genome for homologs of proteins in the STRIPAK and FAR complexes. We found single homologs of both *S. cerevisiae FAR8* (striatin) and *FAR9/10* (SLMAP) in the *N. crassa* genome, which we named *hyphal anastomosis-3* and *4*. Mutations in *ham-3* and *ham-4* result in strains that lack vegetative hyphal fusion, similar to the previously identified *ham-2* mutant. In contrast to the pleiotropic phenotype of the *ham* mutants in *N. crassa*, the *S. cerevisiae FAR* mutants (even the sixtuple mutant) have a subtle-G1 arrest phenotype, but no apparent defect in mating-cell fusion (Kemp and Sprague, 2003), the only type of fusion in yeast. As with *S. cerevisiae*, the *N. crassa ham* mutants can also undergo sexual cell fusion. These data indicate that there are differences between the signal transduction pathways involved in sexual and vegetative fusion in *N. crassa*. However, a *N. crassa* strain containing a deletion of a gene (*Prm-1*), which was shown to be required for plasma membrane fusion during mating-cell fusion in *S. cerevisiae* (Heiman and Walter, 2000), has a nearly identical cell fusion defect during both mating and vegetative fusion in *N. crassa* (Fleissner et al., 2009a) showing that some machinery is required for both cell fusion processes. In addition to vegetative fusion defects, the

ham mutants showed growth and conidiation defects, as well as vacuolar and meiotic/ascospore abnormalities, suggesting that the HAM proteins are involved in biological processes in addition to vegetative cell fusion.

We predict that HAM-2, HAM-3 and sometimes HAM-4 work in a complex involved in cell–cell signaling between germlings and between vegetative hyphae to promote cell fusion. In humans, striatin (*ham-3*) interacts with STRIP1/2 (*ham-2*), mob3 (*mob-3*), the CCM3 and GCK-III kinases, but only sometimes with SLMAP (*ham-4*) (Baillat et al., 2001; Goudreault et al., 2008). Mutations in *N. crassa mob-3* result in mutants that fail to undergo hyphal fusion (Maerz et al., 2009). These data suggest that MOB-3 may also interact with HAM-3 and/or HAM-4. In human endothelial cells, striatin (similar to HAM-3) is responsible for localizing estrogen receptors to caveolae on the cell membrane, inducing the rapid activation of a MAP kinase (Qing et al., 2004). A MAP kinase, MAK-2, is required for vegetative cell fusion in *N. crassa* (Pandey et al., 2004). Recent work has shown that MAK-2 oscillates between the fusion tip and the cytoplasm in germlings undergoing chemotropic interactions (Fleissner et al., 2009b). A second protein, SO, oscillates in opposition to MAK-2; *so* mutants are also fusion defective (Fleissner et al., 2005). Similar to *mak-2* and *so* mutants, *ham* mutants lack any chemotropic interactions (Roca et al., 2005) (this study). We hypothesize that HAM-3 and other HAM proteins play an important role in facilitating the rapid oscillation of MAK-2 and SO proteins at the two opposing sites of cell fusion.

Striatin has been implicated in other signal transduction and cellular processes in mammalian cells, including vesicular trafficking, endocytosis and epithelial cell sheet movement (reviewed in Benoist et al. (2006)). Striatin is involved in a Ca^{2+} signal transduction pathway in which calcium binds striatin via calmodulin; in the absence of calcium, striatin binds directly to caveolin, but moves to the cytoplasm upon stimulation by Ca^{2+} (Gaillard et al., 2001). It has been shown that calcium signaling is involved in fungal hyphal tip growth and establishment (Torralba and Heath, 2001). We predict that calcium signaling will also be required for hyphal fusion through and interaction between calmodulin and HAM-3. Further research will elucidate interactions between HAM-3, calcium signaling, hyphal fusion and MAK-2 activation.

In *S. macrospora*, a close relative to *N. crassa*, mutations in the striatin-like protein *Pro11* resulted in a block in perithecial development (Poggeler and Kuck, 2004). These observation are consistent with our findings in *N. crassa* where mating-cell fusion was observed in *ham-3* crosses, but subsequent perithecial development was blocked, a phenotype that was complemented in a heterokaryon with a^{m1}. Similar to *N. crassa ham-3* and *S. macrospora* (Pro11) mutants, FSR-1 (a striatin-like protein) mutants in *Fusarium verticilliodies* and *F. graminarium* (Shim et al., 2006) also showed defects in female fertility. Both the *ham-3* and *ham-2* mutants show a similar defect in perithecial development following fertilization, while the *ham-4* mutants did not, and were indistinguishable from WT in this regard.

SLMAP, Far9/10 and HAM-4 proteins contain an FHA domain, a phosphoprotein interaction domain, which binds specific phosphothreonine epitopes and is found in many proteins with diverse functions (many involved in cell cycle control) (Durocher and Jackson, 2002). Based on analysis of the *ham-4* RIP mutants, the FHA domain of HAM-4 is sufficient for cell fusion, albeit at a reduced efficiency, suggesting that HAM-4 may recognize a phosphorylated protein during the hyphal fusion process. In humans, SLMAP (*ham-4*), is necessary for myoblast cell fusion during muscle development (Guzzo et al., 2004). Our results showing the inability of *ham-4* deletion mutants to undergo hyphal fusion raise the possibility of a conserved or similar function between SLMAP and *ham-4* in cell fusion.

In *S. cerevisiae*, the Far mutants cannot maintain cell cycle arrest when exposed to mating pheromone but they are unaffected in ascospore development (Kemp and Sprague, 2003). In contrast, all of the *ham* mutants in *N. crassa* show defects in meiotic progression during ascospore formation. Acriflavine staining of developing asci showed that mutations in *ham-2*, *3* and *4* affect nuclear division during ascus development, suggesting that the HAM proteins could also be involved in cell cycle regulation. However, the defect of the *ham* mutants appears to be specific to meiosis, as staining of nuclei in mitotic vegetative cells failed to reveal any differences from WT (data not shown).

Many mutants aberrant in meiosis, ascus development, and ascospore formation have been identified and characterized in *N. crassa* (reviewed in Raju (1992)). Of particular interest and relevance are mutants where meiosis and ascospore delimitation are decoupled, such as those identified in *P. anserina* (Zickler and Simonet, 1980) and *S. cerevisiae* (Moens et al., 1974). When meiosis is uncoupled from ascospore formation, the resulting cross produces a reduced number of spores per ascus and often misshapen spores or spores of the wrong size. For example, an *N. crassa* mutant called *fourspore* (*fsp*) is delayed in mitosis after meiosis II and spores delimit around the four nuclei resulting in only four spores (Raju, 1986b), although occasionally only three spores develop resulting in one large spore and two smaller ones. This phenotype is similar to some of the asci and ascospores from the *ham* homozygous crosses where a decreased number of ascospores per ascus and larger than normal ascospores were observed. However, ascospores from *ham* homozygous crosses often had tails or appendages, and were osmotically sensitive, phenotypes that have not been reported in any other meiotic mutants.

In addition to meiotic/ascospore defects and hyphal fusion defects, the *ham* mutants show aberrant vacuolar morphology. Two of the FAR mutants, *far11* and *far9*, where identified in *S. cerevisiae* using a genome – wide screen for mutants that aberrantly secrete vacuolar-localized carboxy peptidase Y (Bonangelino et al., 2002). Vacuolar morphology has been described in several ascomycete species (Raymond et al., 1992; Oka et al., 2004; Tarutani et al., 2001; Shoji et al., 2006) and the mycorrhizal basidiomycete species *Pisolithus tinctorius* (Allaway and Ashford, 2001). Interestingly, while *vps* mutants do not affect the cellular shape of *S. cerevisiae*, mutations in homologs of *vps* genes in filamentous fungi impact morphology; several *vps* mutants in *A. nidulans* and *A. oryzae* grow slowly or have altered conidiation or branching patterns (Ohneda et al., 2005; Oka et al., 2004). In filamentous fungi, different cell types also display different vacuolar morphology. For example, large vacuoles are found in older hyphae, while small vacuoles are observed in conidia (Shoji et al., 2006). The aberrant vacuoles found in the *ham* mutants, which serve as a storage compartment of Ca^{2+} in fungi (Miller et al., 1990), may be due to sorting defects or a defect in Ca^{2+} signaling, which appears to involve striatin (Gaillard et al. 2001).

Our phenotypic analysis of the *ham-2*, *3* and *4* mutants supports the hypothesis that these proteins function together to regulate germling and hyphal fusion, perhaps in conjunction with MOB-3. Similar to STRIPAK complex identified in humans, it is likely that these proteins form complexes with different sets of proteins to regulate growth, hyphal fusion and sexual development, consistent with the complex pleiotropic phenotype associated with the *ham* mutants. Further genetic and biochemical analyses are required to define the function of these signaling complexes in growth and reproduction in filamentous fungi.

Acknowledgments

We thank Dr. Andre Fleissner for preliminary analysis of the *ham-3*::*hph* mutant and preliminary trichogyne assay analysis in

the *ham-3* and *ham-4* mutants. We also thank Dr. Abigail Leeder for help with the figures and thank the members of the Glass lab for their helpful insights and comments. This work was funded by a National Science Foundation Grant to N.L.G. (MCB-0817615).

References

Allaway, W.G., Ashford, A.E., 2001. Motile tubular vacuoles in extramatrical mycelium and sheath hyphae of ectomycorrhizal systems. Protoplasma 215, 218–225.

Altschul, S., Madden, T., Schaffer, A., Zhang, J., Zhang, Z., Miller, W., Lipman, D., 1997. Gapped BLAST and PSI-BLAST: a new generation of protein database search programs. Nucleic Acids Res. 25, 3389–3402.

Baillat, G., Moqrich, A., Castets, F., Baude, A., Bailly, Y., Benmerah, A., Monneron, A., 2001. Molecular cloning and characterization of phocein, a protein found from the Golgi complex to dendritic spines. Mol. Biol. Cell 12, 663–673.

Bartoli, M., Monneron, A., Ladant, D., 1998. Interaction of calmodulin with striatin, a WD-repeat protein present in neuronal dendritic spines. J. Biol. Chem. 273, 22248–22253.

Benoist, M., Gaillard, S., Castets, F., 2006. The striatin family: a new signaling platform in dendritic spines. J. Physiol. – Paris 99, 146–153.

Bistis, G.N., 1981. Chemotropic interactions between trichogynes and conidia of opposite mating-type in *Neurospora crassa*. Mycologia 73, 959–975.

Bistis, G.N., 1983. Evidence for diffusable mating-type specific trichogyne attactants in *Neurospora crassa*. Exp. Mycol. 7, 292–295.

Bonangelino, C., Chavez, E., Bonifacino, J., 2002. Genomic screen for vacuolar protein sorting genes in *Saccharomyces cerevisiae*. Mol. Biol. Cell 13, 2486–2501.

Brockman, H.E., de Serres, F.J., 1963. "Sorbose toxicity" in Neurospora. Am. J. Bot. 50, 709–714.

Buller, A.H.R., 1933. Researches on Fungi, vol. 5. Longman, London.

Castets, F., Bartoli, M., Barnier, J., Baillat, G., Salin, P., Moqrich, A., Bourgeois, J., Denizot, F., Rougon, G., Calothy, G., et al., 1996. A novel calmodulin-binding protein, belonging to the WD-repeat family, is localized in dendrites of a subset of CNS neurons. J. Cell Biol. 134, 1051–1062.

Colot, H.V., Park, G., Turner, G.E., Ringelberg, C., Crew, C.M., Litvinkova, L., Weiss, R.L., Borkovich, K.A., Dunlap, J.C., 2006. A high-throughput gene knockout procedure for Neurospora reveals functions for multiple transcription factors. Proc. Natl. Acad. Sci. USA 103, 10352–10357.

Davis, R.H., 2000. Neurospora: Contributions of a Model Organism. Oxford University Press, New York.

Durocher, D., Jackson, S., 2002. The FHA domain. FEBS Lett. 513, 58–66.

Fleissner, A., Diamond, S., Glass, N.L., 2009a. The *Saccharomyces cerevisiae* PRM1 homolog in *Neurospora crassa* is involved in vegetative and sexual cell fusion events but also has postfertilization functions. Genetics 181, 497–510.

Fleissner, A., Leeder, A.C., Roca, M.G., Read, N.D., Glass, N.L., 2009b. Oscillatory recruitment of signaling proteins to cell tips promotes coordinated behavior during cell fusion. Proc. Natl. Acad. Sci. USA 106, 19387–19392.

Fleissner, A., Sarkar, S., Jacobson, D.J., Roca, M.G., Read, N.D., Glass, N.L., 2005. The so locus is required for vegetative cell fusion and postfertilization events in *Neurospora crassa*. Eukaryot. Cell 4, 920–930.

Fleissner, A., Simonin, A.R., Glass, N.L., 2008. Cell fusion in the filamentous fungus, *Neurospora crassa*. Methods Mol. Biol. 475, 21–38.

Freitag, M., Hickey, P.C., Raju, N.B., Selker, E.U., Read, N.D., 2004. GFP as a tool to analyze the organization, dynamics and function of nuclei and microtubules in *Neurospora crassa*. Fungal Genet. Biol. 41, 897–910.

Gaillard, S., Bartoli, M., Castets, F., Monneron, A., 2001. Striatin, a calmodulin-dependent scaffolding protein, directly binds caveolin-1. FEBS Lett. 508, 49–52.

Glass, N.L., Rasmussen, C., Roca, M.G., Read, N.D., 2004. Hyphal homing, fusion and mycelial interconnectedness. Trends Microbiol. 12, 135–141.

Goudreault, M., D'Ambrosio, L.M., Kean, M.J., Mullin, M., Larsen, B.G., Sanchez, A., Chaudhry, S., Chen, G.I., Sicheri, F., Nesvizhskii, A.I., et al., 2008. A PP2A phosphatase high-density interaction network identifies a novel striatin-interacting phosphatase and kinase complex linked to the cerebral cavernous malformation 3 (CCM3) protein. Mol. Cell Proteom. 8, 157–171.

Guzzo, R., Wigle, J., Salih, M., Moore, E., Tuana, B., 2004. Regulated expression and temporal induction of the tail-anchored sarcolemmal-membrane-associated protein is critical for myoblast fusion. Biochem. J. 381, 599–608.

Heiman, M.G., Walter, P., 2000. Prm1p, a pheromone-regulated multispanning membrane protein, facilitates plasma membrane fusion during yeast mating. J. Cell Biol. 151, 719–730.

Higashiyama, T., Kuroiwa, H., Kuroiwa, T., 2003. Pollen-tube guidance: beacons from the female gametophyte. Curr. Opin. Plant Biol. 6, 36.

Kemp, H., Sprague, G., 2003. Far3 and five interacting proteins prevent premature recovery from pheromone arrest in the budding yeast *Saccharomyces cerevisiae*. Mol. Cell Biol. 23, 1750–1763.

Kim, H., Borkovich, K., 2004. A pheromone receptor gene, pre-1, is essential for mating type-specific directional growth and fusion of trichogynes and female fertility in *Neurospora crassa*. Mol. Microbiol. 52, 1781–1798.

Lee, S.B., Milgroom, M.G., Taylor, J.W., 1988. A rapid, high yield mini-prep method for isolation of total genomic DNA from fungi. Fungal Genet. Newslett. 35, 23–24.

Maerz, S., Dettmann, A., Ziv, C., Liu, Y., Valerius, O., Yarden, O., Seiler, S., 2009. Two NDR kinase-MOB complexes function as distinct modules during septum formation and tip extension in *Neurospora crassa*. Mol. Microbiol. 74, 707–723.

Maerz, S., Ziv, C., Vogt, N., Helmstaedt, K., Cohen, N., Gorovits, R., Yarden, O., Seiler, S., 2008. The nuclear Dbf2-related kinase COT1 and the mitogen-activated protein kinases MAK1 and MAK2 genetically interact to regulate filamentous growth, hyphal fusion and sexual development in *Neurospora crassa*. Genetics 179, 1313–1325.

Margolin, B.S., Freitag, M., Selker, E.U., 1997. Improved plasmids for gene targeting at the his-3 locus of *Neurospora crassa* by electroporation. Fungal Genet. Newslett. 44, 34–36.

McCluskey, K., 2003. The Fungal Genetics Stock Center: from molds to molecules. Adv. Appl. Microbiol. 52, 245–262.

Miller, A.J., Vogg, G., Sanders, D., 1990. Cytosolic calcium homeostasis in fungi: roles of plasma membrane transport and intracellular sequestration of calcium. Proc. Natl. Acad. Sci. USA 87, 9348–9352.

Moens, P., Esposito, R., Esposito, M., 1974. Aberrant nuclear behavior at meiosis and anucleate spore formation by sporulation-deficient (SPO) mutants of *Saccharomyces cerevisiae*. Exp. Cell Res. 83, 166–174.

Ohneda, M., Arioka, M., Kitamoto, K., 2005. Isolation and characterization of *Aspergillus oryzae* vacuolar protein sorting mutants. Appl. Environ. Microbiol. 71, 4856–4861.

Oka, M., Maruyama, J., Arioka, M., Nakajima, H., Kitamoto, K., 2004. Molecular cloning and functional characterization of avaB, a gene encoding Vam6p/Vps39p-like protein in *Aspergillus nidulans*. FEMS Microbiol. Lett. 232, 113–121.

Pandey, A., Roca, M.G., Read, N.D., Glass, N.L., 2004. Role of a mitogen-activated protein kinase pathway during conidial germination and hyphal fusion in *Neurospora crassa*. Eukaryot. Cell 3, 348–358.

Perkins, D.D., 1984. Advantages of using the inactive-mating-type a^{m1} strain as a helper component in heterokaryons. Fungal Genet. Newslett. 31, 41–42.

Poggeler, S., Kuck, U., 2004. A WD40 repeat protein regulates fungal cell differentiation and can be replaced functionally by the mammalian homologue striatin. Eukaryot. Cell 3, 232–240.

Primakoff, P., Myles, D.G., 2007. Cell–cell membrane fusion during mammalian fertilization. FEBS Lett. 581, 2174–2180.

Qing, L., Pallas, D., Surks, H., Baur, W., Mendelsohn, M., Karas, R., 2004. Striatin assembles a membrane signaling complex necessary for rapid, nongenomic activation of endothelial NO synthase by estrogen receptor alpha. Proc. Natl. Acad. Sci. USA 101, 17126–17131.

Raju, N.B., 1980. Meiosis and ascospore genesis in Neurospora. Eur. J. Cell Biol. 23, 208–223.

Raju, N.B., 1986a. A simple fluorescent staining method for meiotic chromosomes of *Neurospora*. Mycologia 78, 901–906.

Raju, N.B., 1986b. Ascus development in two temperature-sensitive four-spore mutants of *Neurospora crassa*. Can. J. Genet. Cytol. 28, 982–990.

Raju, N.B., 1992. Genetic control of the sexual cycle in Neurospora. Mycol. Res. 96, 241–262.

Raymond, C.K., Howald-Stevenson, I., Vater, C.A., Stevens, T.H., 1992. Morphological classification of the yeast vacuolar protein sorting mutants: evidence for a prevacuolar compartment in class E vps mutants. Mol. Biol. Cell 3, 1389–1402.

Rayner, A., 1991. The challenge of the individualistic mycelium. Mycologia 83, 48–71.

Rayner, A.D.M., 1996. Interconnectedness and Individualism in Fungal Mycelia. Cambridge University Press, Cambridge.

Read, N.D., Fleißner, A., Roca, M.G., Glass, N.L., 2010. Hyphal fusion. In: Borkovich, K.A., Ebbole, D. (Eds.), Cellular and Molecular Biology of Filamentous Fungi. American Society of Microbiology, pp. 260–273.

Roca, M., Arlt, J., Jeffree, C., Read, N., 2005. Cell biology of conidial anastomosis tubes in *Neurospora crassa*. Eukaryotic. Cell 4, 911–919.

Ryan, F., Beadle, G., Tatum, E., 1943. The tube method of measuring the growth rate of Neurospora. Am. J. Bot. 30, 784–799.

Sambrook, J., Russell, D.W., 2001. Molecular Cloning: A Laboratory Manual. Cold Spring Harbor Laboratory Press, Cold Spring Harbor.

Selker, E.U., 2002. Repeat-induced gene silencing in fungi. Adv. Genet. 46, 439–450.

Shim, W.B., Sagaram, U.S., Choi, Y.E., So, J., Wilkinson, H.H., Lee, Y.W., 2006. FSR1 is essential for virulence and female fertility in *Fusarium verticillioides* and *F. graminearum*. Mol. Plant Microbe Interact. 19, 725–733.

Shiu, P.K.T., Raju, N.B., Zickler, D., Metzenberg, R.L., 2001. Meiotic silencing by unpaired DNA. Cell 107, 905–916.

Shoji, J.Y., Arioka, M., Kitamoto, K., 2006. Vacuolar membrane dynamics in the filamentous fungus *Aspergillus oryzae*. Eukaryot. Cell 5, 411–421.

Smith, T., Gaitatzes, C., Saxena, K., Neer, E., 1999. The WD repeat: a common architecture for diverse functions. Trends Biochem. Sci. 24, 181–185.

Tarutani, Y., Ohsumi, K., Arioka, M., Nakajima, H., Kitamoto, K., 2001. Cloning and characterization of *Aspergillus nidulans* vpsA gene which is involved in vacuolar biogenesis. Gene 268, 23–30.

Torralba, S., Heath, I., 2001. Cytoskeletal and Ca2+ regulation of hyphal tip growth and initiation. Curr. Top. Dev. Biol. 51, 135–187.

Uetz, P., Giot, L., Cagney, G., Mansfield, T., Judson, R., Knight, J., Lockshon, D., Narayan, V., Srinivasan, M., Pochart, P., et al., 2000. A comprehensive analysis of protein–protein interactions in *Saccharomyces cerevisiae*. Nature 403, 623–627.

Vignery, A., 2008. Macrophage fusion: molecular mechanisms. Methods Mol. Biol. 475, 149–161.

Vogel, H.J., 1956. A convenient growth medium for Neurospora. Microbiol. Genet. Bull. 13, 42–46.
Westergaard, M., Mitchell, H.K., 1947. Neurospora V. A synthetic medium favoring sexual reproduction. Am. J. Bot. 34, 573–577.
Wurmser, A., Sato, T., Emr, S., 2000. New component of the vacuolar class C-Vps complex couples nucleotide exchange on the Ypt7 GTPase to SNARE-dependent docking and fusion. J. Cell Biol. 151, 551–562.
Xiang, Q., Rasmussen, C., Glass, N.L., 2002. The ham-2 Locus, encoding a putative transmembrane protein, is required for hyphal fusion in *Neurospora crassa*. Genetics 160, 169–180.
Zeng, Z.-Y., Chen, J.-M., 2009. Cell–cell fusion: human multinucleated osteoclasts. Cent. Eur. J. Biol. 4, 543–548.
Zickler, D., Simonet, J., 1980. Identification of gene-controlled steps of ascospore development in *Podospora anserina*. Exp. Mycol. 4, 191–206.